Proceedings of ASME 2018
International Mechanical Engineering Congress and Exposition
IMECE2018
November 9-15, 2018, Pittsburgh, PA, USA

IMECE2018-87751

FINITE ELEMENT ANALYSIS OF THE PASSENGER RAIL EQUIPMENT WORKSTATION TABLE SLED TEST

Shaun Eshraghi
Volpe National Transportation Systems Center
Cambridge, MA, USA

Kristine Severson
Volpe National Transportation Systems Center
Cambridge, MA, USA

David Hynd
Transport Research Laboratory
Wokingham, Berkshire, UK

A. Benjamin Perlman
Volpe National Transportation Systems Center
Cambridge, MA, USA

ABSTRACT

Fixed workstation tables in passenger rail coaches can pose a potential injury hazard for passengers seated at them during an accident. Tables designed to absorb impact energy while minimizing contact forces can reduce the risk of serious injury, while helping to compartmentalize occupants during a train collision. The Rail Safety and Standards Board (RSSB) in the U.K. issued safety requirement GM/RT2100, Issue 5 [1] and the American Public Transportation Association (APTA) in the U.S. issued safety standard APTA PR-CS-S-018-13, Rev. 1 [2] with the goals of setting design and performance requirements for energy-absorbing workstation tables.

The U.S. Department of Transportation, Federal Railroad Administration (FRA) Office of Research, Development and Technology directed the Volpe National Transportation Systems Center (Volpe Center) to evaluate the performance of the Hybrid-III Rail Safety (H3-RS) anthropomorphic test device (ATD), also known as a test dummy, in the APTA sled test in order to incorporate a reference to the H3-RS in the safety standard. The Volpe Center contracted with the manufacturer of the H3-RS, Transport Research Laboratory (TRL), in the U.K. to conduct a series of sled tests [3] with energy-absorbing tables, donated by various table manufacturers. The tables were either already compliant with the RSSB table standard or were being developed to comply with the APTA table standard.

The sled test specified in Option A of the APTA table standard involves the use of two different 50th percentile male frontal impact ATDs. The H3-RS and the standard Hybrid-III (H3-50M) ATDs performed as expected. The H3-RS, which features bilateral deflection sensors in the chest and abdomen, was able to measure abdomen deflections while the H3-50M, which features a single sensor measuring chest compression, was not equipped to measure abdomen deflection.

This study attempts to validate a finite element (FE) model of the APTA 8G sled test with respect to the thorax response of the H3-RS and H3-50M. The model uses a simplified rigid body-spring representation of one of the energy absorbing tables tested by TRL. The FE models of the H3-RS ATD and the H3-50M ATD were provided by TRL and LSTC, respectively. Results from the sled tests and FE simulations are compared using data obtained from the chest accelerometer, the chest and abdomen deflection sensors, and the femur load cells. Using video analysis, the gross motion of the dummies and table are also compared. Technical challenges related to model validation of the 8G sled test are also discussed.

This study builds on previous analyses conducted to validate the abdomen response of the H3-RS FE model, which are presented in a companion paper [4].

INTRODUCTION

The APTA table standard for passenger railroad equipment [2] was first published in March 2013. The performance requirements in the APTA standard are based on quasi-static and dynamic [5] test results using an FRA prototype table, and sled test simulations [6] conducted using MADYMO (a multibody system solver distributed by TASS International) [7]. Subsequently, railroad operators started to include the standard in their technical specifications for new equipment procurements. Table manufacturers have been researching and developing new table designs that are compliant with the standard. However, the 8G dynamic sled test scenario specified in the APTA standard is a challenging loading environment in which a large portion of the impact load from the edge of the workstation table is concentrated on the soft abdomen of the ATD.

The APTA standard allows compliance to be demonstrated using one of two options. Option A requires an 8G sled test using a frontal impact ATD capable of measuring abdomen deflection seated in the wall seat, where contact forces are typically highest, and a standard H3-50M ATD seated in the aisle seat. Option A imposes limits on the abdomen and chest deflection to 67 and 63 mm, respectively.

In Option B of the standard, the sled test can be performed with two standard H3-50M ATDs, which measure chest deflection at one location, but are not equipped to measure abdomen deflection. In lieu of measuring abdomen deflection, a destructive quasi-static test is required in addition to the 8G sled test. At each seat position, the quasi-static test has an energy absorption requirement of 706 J (6,250 in-lb_f) with a load limit of 10 kN (2,250 lb_f). The energy absorption and load limit requirements were developed from the results of a previous parametric study [6]. Options A and B are intended to provide equivalent safety.

In addition to the requirements focusing on limiting the risk of injury for occupants seated in forward-facing seats, the APTA standard also requires that the longitudinal space remaining between the table edge and the opposite seat after sled testing is no less than 15 inches. The space requirement is intended to minimize injury to the rear-facing passengers due to table contact and to permit egress post-accident. This space requirement reduces the distance available for table displacement, which is used in several designs to absorb energy and minimize abdominal loads.

Finite element analysis is a useful tool to study the dynamic sled test environment in order to better understand the injury risks posed by workstation tables. However, the FE model of the dynamic sled test must first be validated to develop confidence in the models of both the ATDs and the tables.

In the companion paper [4], the authors validated the abdominal response of the H3-RS FE model using 12 different pendulum impactor tests. In this study, the response of both ATDs is validated using the APTA 8G dynamic sled test and a specific energy absorbing table design (identified as Table IV previously [3]). This particular table design was chosen because it could be modeled using a simplified rigid body-spring representation and because it was the only table tested [8] that met the quasi-static energy absorption requirements as described in the next section. A pre-test photo of the sled test setup with the energy absorbing table, referred to as the Type IV table, is shown in Figure 1 and the corresponding FE model is shown in Figure 2.

Figure 1. Dynamic Sled Test Setup with Type IV Table and H3-RS in Wall Seat and H3-50M Seated in Aisle Seat [3]

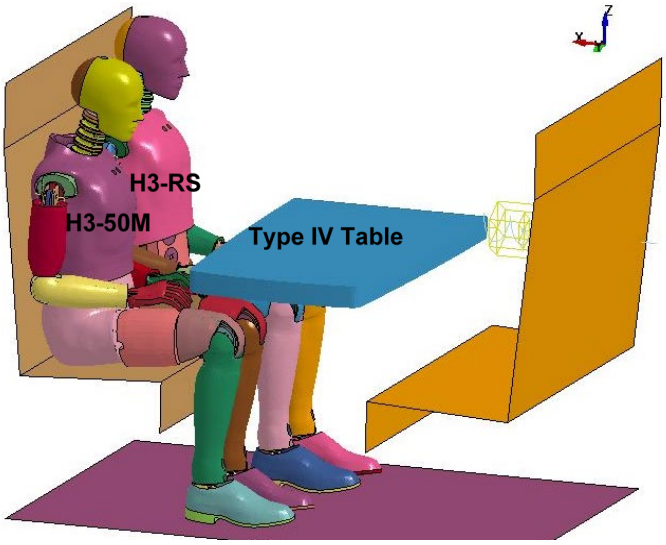

Figure 2. FE Model of Sled Test (Isometric View)

After validating the FE model of the dynamic table test, the authors intend to examine the various APTA requirements such as the quasi-static load and energy absorption requirements (Option B) and the longitudinal space requirement (Options A and B). There is also interest in conducting sensitivity studies on other test conditions such as table height and crash pulse magnitude.

METHODS

Quasi-static Test

The Volpe Center contracted with Sharma & Associates, Inc. to conduct quasi-static destructive testing [8], according to Option B of the APTA table standard, on two table designs that were evaluated in sled testing by TRL. The quasi-static test involves loading the table simultaneously with two rigid indenter blocks (Figure 3) at a rate of 50 mm/minute until each indenter reaches 10 kN (2,250 lb_f). A photo taken during quasi-static testing of the Type IV table is shown in Figure 4.

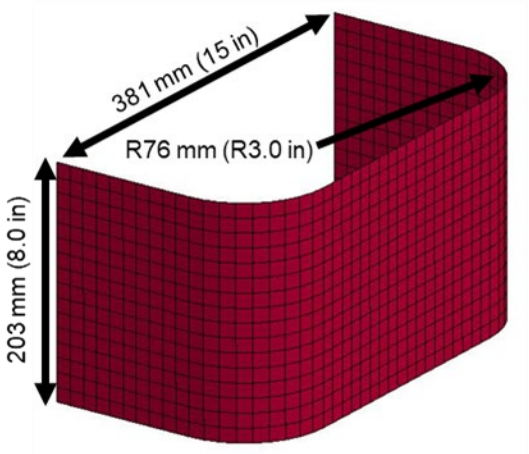

Figure 3. FE Model of Rigid Indenter Block Used in Quasi-static Testing

Figure 4. Photograph during Quasi-static Testing

The quasi-static force versus crush response of Table IV was used to calibrate the response of a simple rigid body-spring FE model of the table. An inelastic translational spring element (crush spring) attached to the wall side, center of the table was used with the characteristic shown in Figure 5. An inelastic rotational spring (torque spring) also attached to the wall side, center of the table with the response shown in Figure 6 was used to model the rotation of the table. For the purpose of this study, the authors use a simplified representation of a manufacturer's table for validation since the goal is not to evaluate the manufacturer's table design.

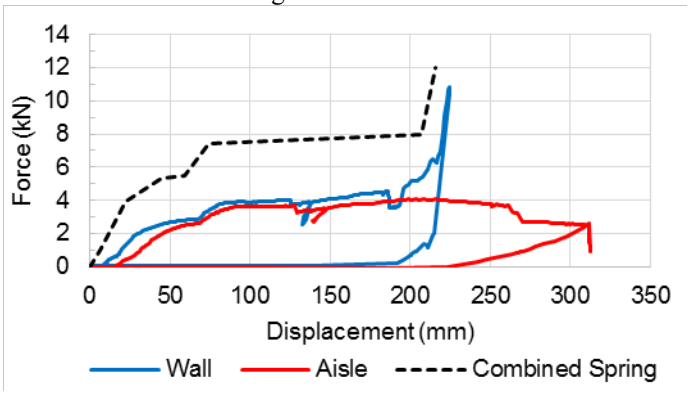

Figure 5. Force-Displacement Response of Type IV Table in Quasi-static Testing and Crush Spring Definition

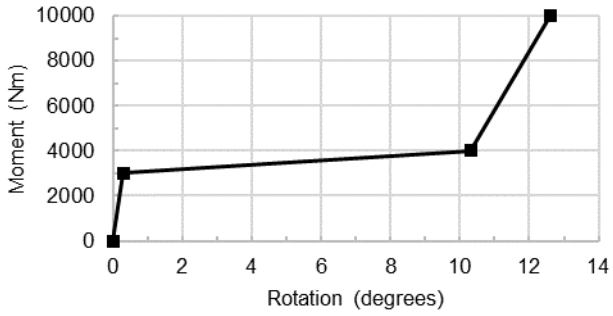

Figure 6. Torque Spring Definition

Sled Test

The H3-RS and H3-50M FE models were positioned on the forward-facing seat using LS-PrePost® V4.2. The initial positioning of the ATDs is shown in Figure 2 and Figure 7. Automatic contact definitions were assigned between the ATDs and the table as well as the floor with a static coefficient of friction of 0.2.

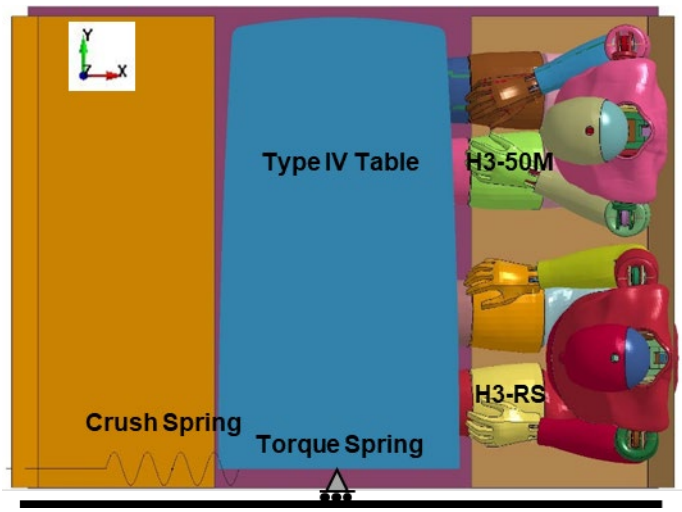

Figure 7. FE Model of Sled Test (Top View)

After reviewing the videos of the sled test, it was determined that the only seat contact that played a significant role in the motion of the ATDs was with the seat bottom frame of the opposing seats where the knees made contact. A rigid-body-one-way contact definition was assigned to the seat frame with the simple piecewise-linear force-displacement response shown in Figure 8 and a damping coefficient of 0.25 kg/ms. This characteristic is not based on the material properties of the seat but was calibrated post-test to capture the gross motion of the ATDs. A similar approach has been used previously by the authors to model table impacts [6, 9, 10, 11].

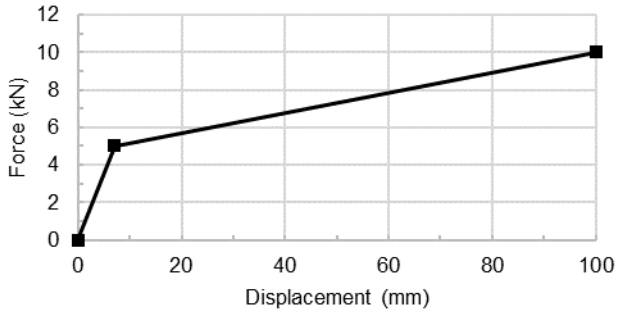

Figure 8. Force-displacement Contact Response of Rear-facing Seat Bottom Cushion

The measured test crash pulse, shown in Figure 9, was applied as a longitudinal body acceleration to the ATDs in order to simulate the sled motion. In testing, there was difficulty achieving the idealized triangular pulse duration so the test laboratory increased the magnitude to reach a change in velocity that was within 5% of the target (9.8 m/s).

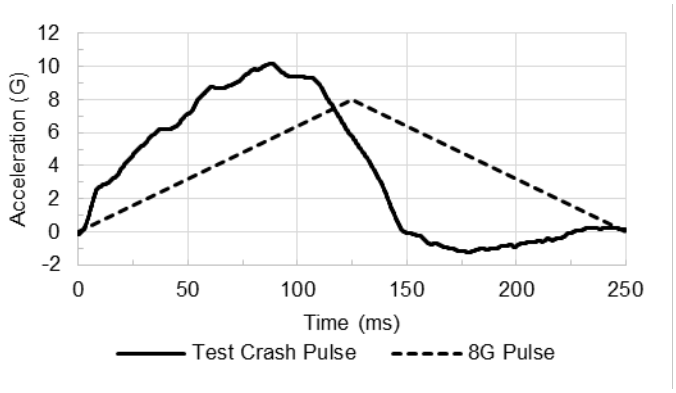

Figure 9. APTA 8 g Crash Pulse and Test Crash Pulse (CFC 60)

A gravity ramp was applied from 0G to 1G from 100 ms to 150 ms in order to capture the settling of the ATDs after the ATDs initially contact the table at approximately 100 ms. Gravity was not applied before the ATDs' impact with the table at 100 ms so that the vertical alignment between the ATDs and table remained unchanged.

The chest and abdomen deflection sensors in the H3-RS are described in the companion paper [4]. The thorax of the H3-50M ATD has only one sensor, located behind the sternum, which measures chest compression.

Test data acquired from the ATDs and the corresponding FE model outputs were digitally filtered in accordance with *SAE J211-1 Instrumentation for Impact Test* [12] using channel frequency class (CFC) filters. The chest accelerometer test data were filtered with a CFC 180 filter. The chest and abdomen deflection and femur load data were filtered using a CFC 600 filter. The pelvis accelerometer test data were filtered with a CFC 1000 filter.

In order to validate the FE model, the following measurements were compared with test data: (1) peak longitudinal deflections from the thoracic deflection sensors; (2) resultant chest and pelvis accelerations; and (3) femur axial load.

RESULTS

The motion of the ATDs in the FE model correlated well with observations from high speed video up to 200 ms as seen in Figure 10 and Figure 11. The contact stiffness for the opposing seat was specified uniformly over the surface, but the physical seats are not expected to have a uniform stiffness as they have a transverse structural member at the bottom of the seat cushion. The H3-50M can be seen overriding this member in the test video but not in the FE model.

The settling of the ATDs after the impact was not accurately captured by the current FE model. The peak chest and abdomen deflections occur around 175 ms so the ability to capture the motion of the ATDs up to 200 ms was deemed acceptable for the purpose of this study.

Chest Deflection – H3-RS

It was observed that the peak chest deflections measured in the sled test were in reasonable agreement with the H3-RS FE model as can be seen in Figure 12. In testing, the lower chest peak deflections were above the APTA limit of 63 mm in both the left (72 mm) and right (69 mm) CRUX sensors; however, the simulated lower chest peak deflections on the left (70 mm) was above the limit and the right (61 mm) was below the limit. The chest deflection in the simulations was slightly underestimated in all four CRUX sensors.

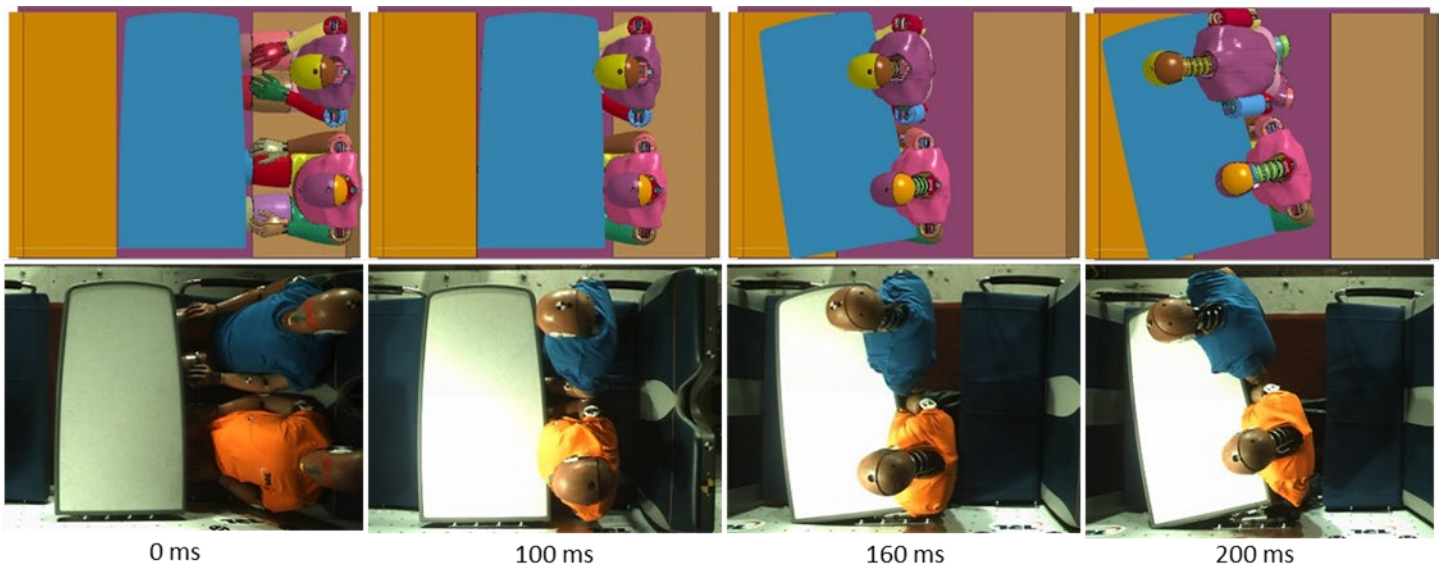

Figure 10. Top View Comparison of FE Model with Sled Test Video

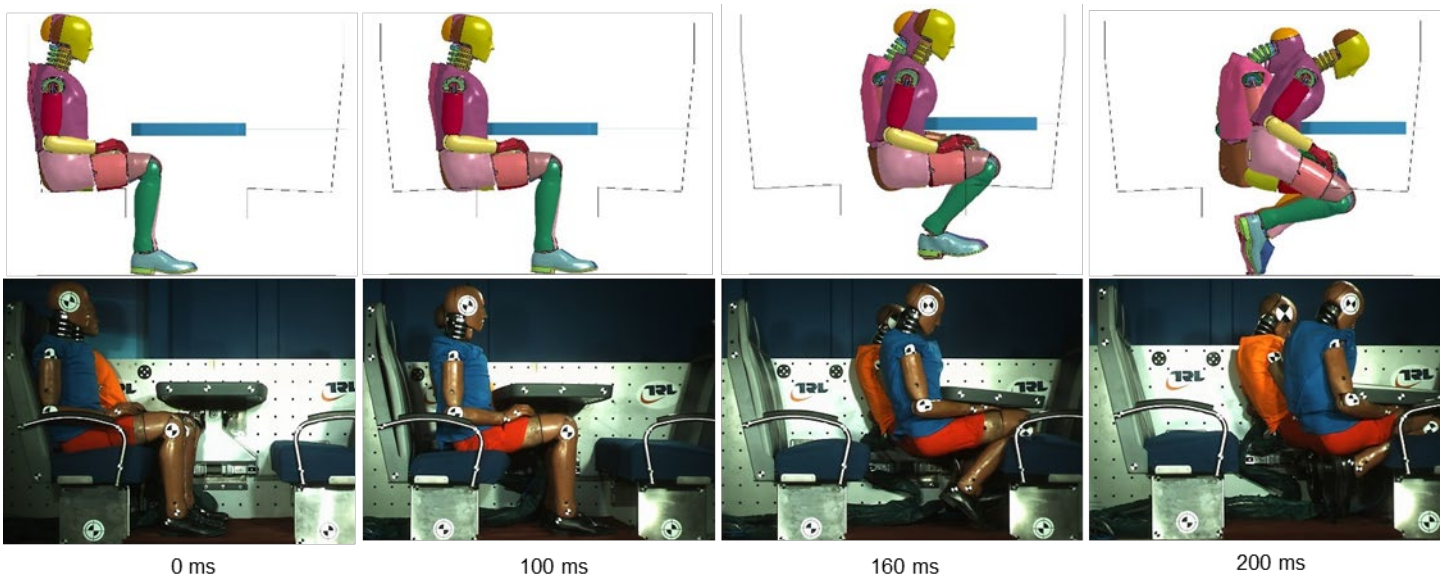

Figure 11. Side View Comparison of FE Model with Sled Test video

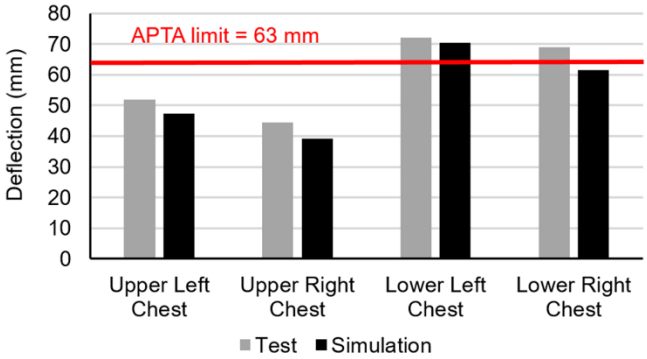

Figure 12. H3-RS Peak Chest Deflections

The qualitative shape and phase of the upper and lower chest deflection time-histories were also in reasonable agreement as can be seen in Figure 13 and Figure 14. In both the test and model, chest deflection initiated at 100 ms which is immediately after the peak sled acceleration (Figure 9). The chest deflection then plateaued from 125 to 140 ms, corresponding to the plateau force observed in quasi-static testing (Figure 5), and the peak occurred at approximately 170 ms.

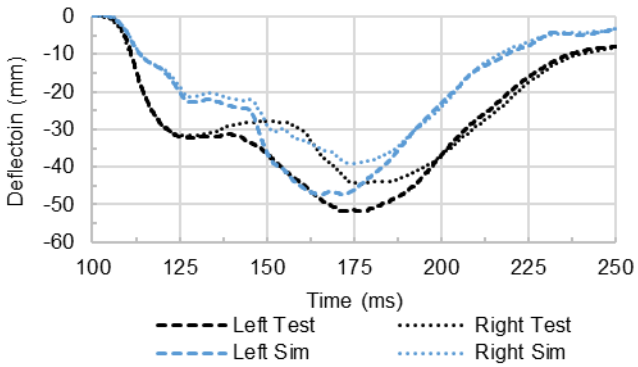

Figure 13. H3-RS Upper Chest Deflection (CFC 600)

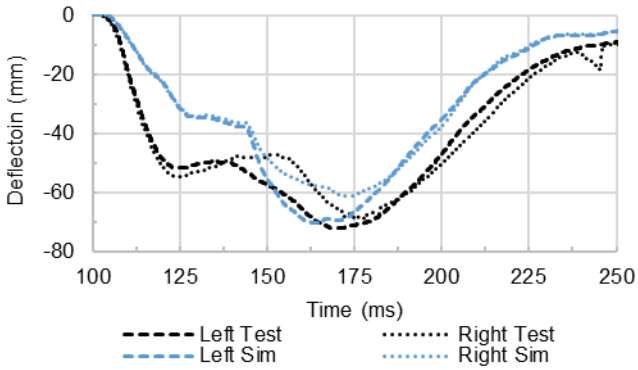

Figure 14. H3-RS Lower Chest Deflection (CFC 600)

Abdomen Deflection – H3-RS

The peak H3-RS abdomen deflections did not correlate as well as the chest deflections, as shown in Figure 15. In testing,

the abdomen deflections all met the APTA limit of 67 mm, except the upper right abdomen DGSP which experienced an instrumentation failure and was omitted. In the FE model, the upper left abdomen deflection (48 mm) was 18% lower than in testing.

The qualitative shape and phase of the upper abdomen deflection time-histories were in reasonable agreement, as shown Figure 16. However, the lower abdomen time-histories did not correlate as well, as shown in Figure 17. In this case, test results did not match with the expectation that the left peak deflection would be higher than the right because the table is effectively stiffer on that side where it is mounted to the wall.

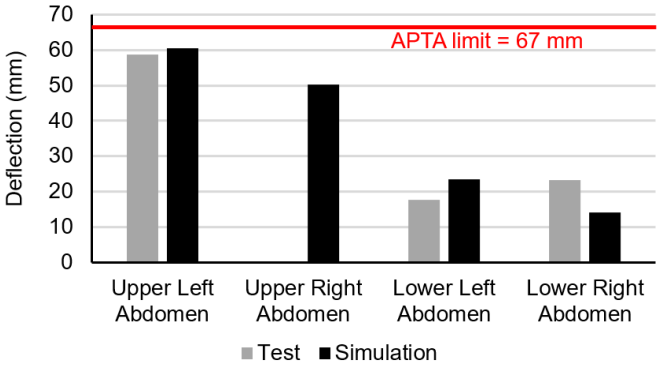

Figure 15. H3-RS Peak Abdomen Deflections with Upper Right Sensor Omitted Due to Instrumentation Failure

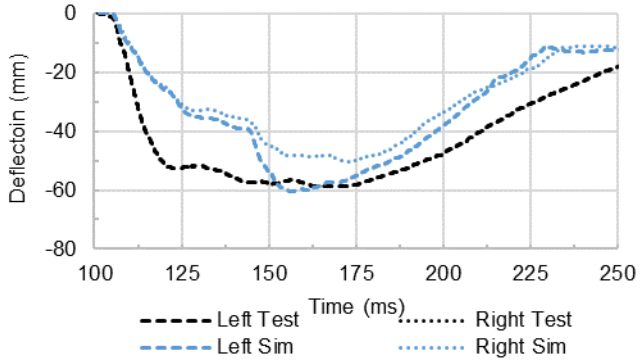

Figure 16. H3-RS Upper Abdomen Deflection with Right Sensor Omitted Due to Instrumentation Failure (CFC 600)

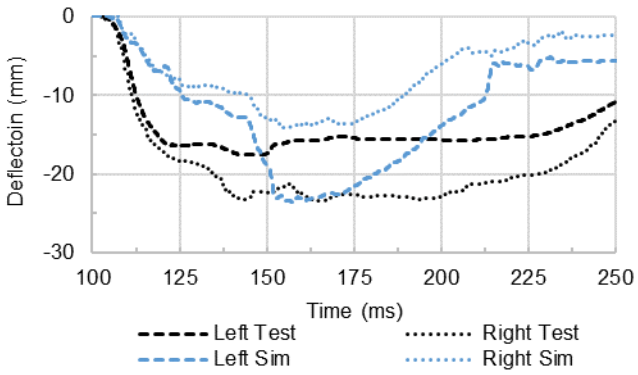

Figure 17. H3-RS Lower Abdomen Deflection (CFC 600)

Chest Deflection – H3-50M

The FE model qualitatively captured the chest deflection behavior in the H3-50M ATD as can be seen in Figure 18. The peak deflection was 59 mm in test and 67 mm in the FE model. The model does not capture the unexpected drop in chest deflection at 170 ms. It is possible that this dip in deflection was caused by rotation of the table about the lateral axis which is not specified in the model.

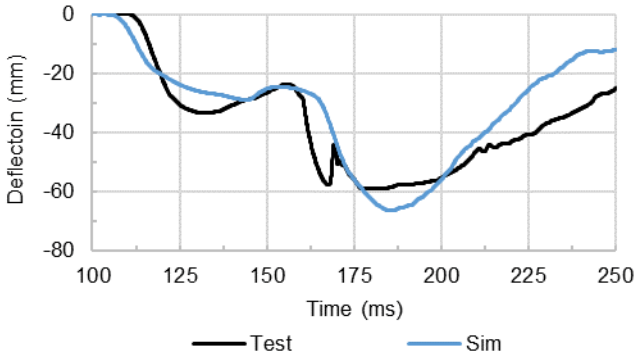

Figure 18. H3-50M Chest Deflection (CFC 600)

Chest Acceleration

The resultant chest acceleration for the H3-RS was slightly out of phase with the model (Figure 19). However the peak resultant accelerations were in agreement at approximately 32G.

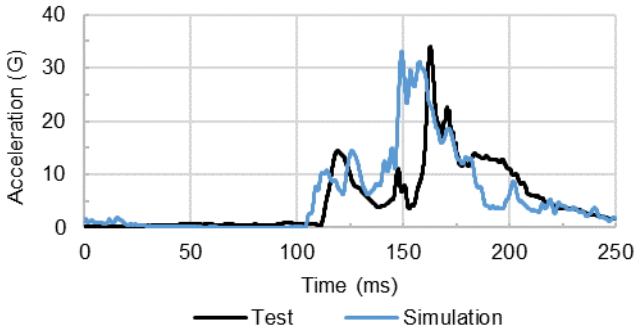

Figure 19. H3-RS Chest Acceleration Resultant (CFC 180)

The resultant chest acceleration for the H3-50M ATD was also slightly out of phase and showed poorer agreement than the H3-RS ATD for the peak resultant acceleration. Also, there was an initial spike in resultant acceleration at 115 ms in the test that was not captured in the model.

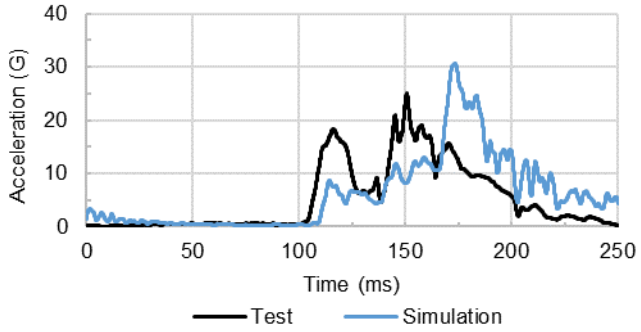

Figure 20. H3-50M Chest Acceleration Resultant (CFC 180)

Pelvis Acceleration

The resultant pelvis acceleration for the H3-RS showed better agreement in phase than the resultant chest acceleration but worse agreement in shape. The peak acceleration at 145 ms was sustained longer in the simulation. The acceleration stayed above 20G for approximately 20 ms for both ATDs. For the H3-50M, a secondary peak was observed in the model at 195 ms that was not seen in the test results and is related to H3-50M pitching forward in the model.

The disagreement in the pelvis acceleration test and model results is due to the simplified representation of the ATDs contact with the rear-facing seat bottom cushion using a rigid-body-one-way contact definition (force-displacement response shown in Figure 8). It is expected that a deformable model of the opposite seat with automatic contact would show better agreement and this is an area of future work.

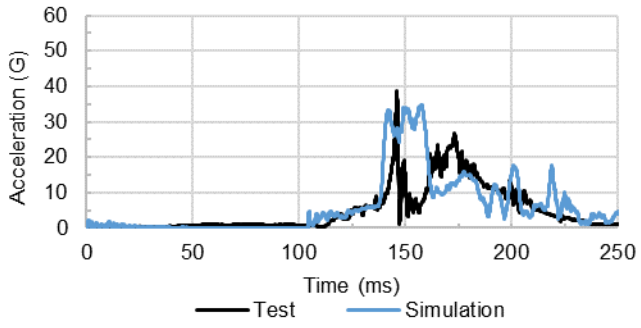

Figure 21. H3-RS Pelvis Acceleration Resultant (CFC 1000)

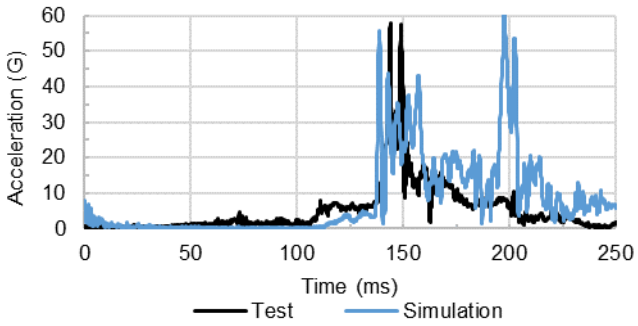

Figure 22. H3-50M Pelvis Acceleration Resultant (CFC 1000)

Femur Loads

The peak magnitudes of the femur forces for the H3-RS (Figure 23) and H3-50M (Figure 24) ATDs were in agreement at 4 – 6 kN except for the left femur of the H3-50M. The test data for the left femur did not show a peak near 150 ms as expected, and it is possible that this sensor malfunctioned during the test. It can be seen that the femur load in the FE model is sustained for a much longer duration than in the test. Perfect agreement for the femur load results was not anticipated and will be rectified with a deformable model of the rear-facing seat bottom cushion.

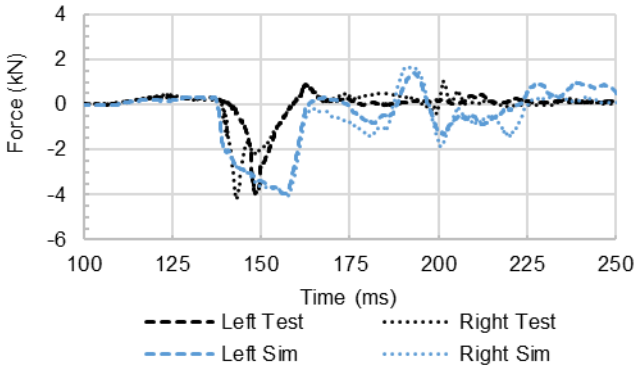

Figure 23. H3-RS Femur Loads (CFC 600)

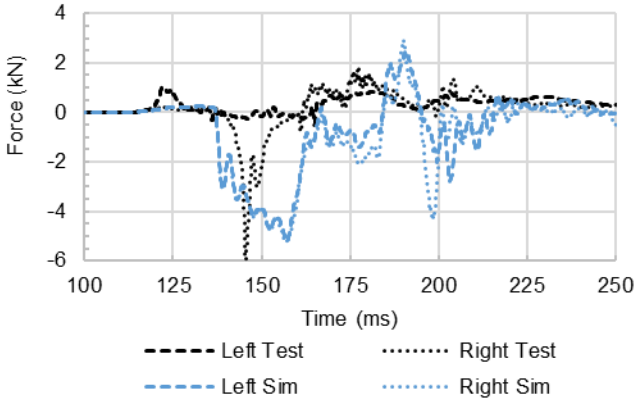

Figure 24. H3-50M Femur Loads (CFC 600)

Table Loads

The rigid body-spring representation of the energy absorbing table features a translational crush spring and a rotational torque spring attached to the wall side center of the table. These springs are not present in the physical table so they cannot be validated against real measurements; however, they are presented here to study the behavior of the simplified table model.

A peak force of approximately 15 kN (2,922 lb_f) at 165 ms was observed in the crush spring as shown in Figure 25. The total energy absorption (longitudinal work) from the crush spring was approximately 1,398 J (12,373 in-lb_f), which corresponds with the summed 1,412 J (12,500 in-lb_f) energy absorption requirement (from both loading rams in the quasi-static test) using Option B of the APTA standard.

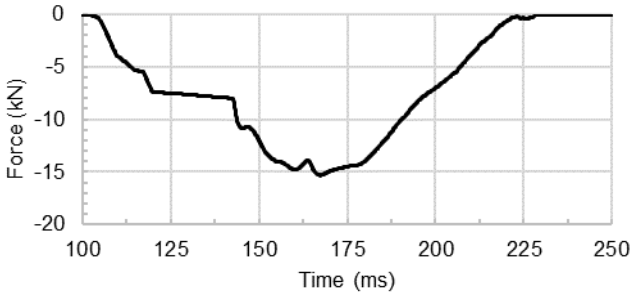

Figure 25. Table Model Crush Spring Force

The rotational spring reached a peak moment of approximately 8,034 Nm (5,926 lb_f-ft) at 185 ms as can be seen in Figure 26. The total rotational work from the spring was approximately 717 J (6,345 in-lb_f).

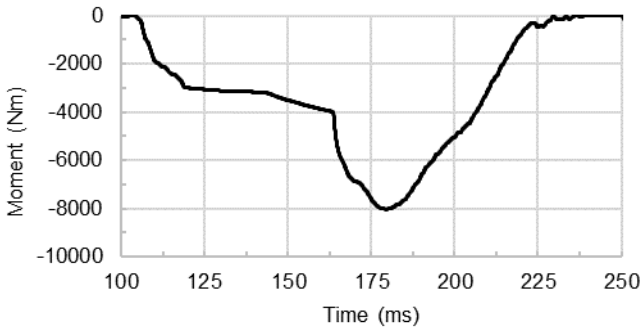

Figure 26. Table Model Torque Spring Moment of Force

DISCUSSION

The 8G sled test model captured the gross motions of the table and ATDs and gave reasonable values for energy absorption. It is promising that the H3-RS ATD peak chest deflections in the FE model and the test were similar. However, the abdomen deflection sensors in the H3-RS FE model and test were not in very good agreement.

Positioning of the H3-RS and H3-50M ATDs proved difficult in the FE model. The chest and abdomen deflections are sensitive to changes in impact location in the vertical direction. Pendulum impact testing at various heights [13] and FE analysis performed in this study's companion conference paper have shown that the area near the lower ribs and upper abdomen is especially sensitive to impact height. In the case of the sled tests, the tables were positioned at heights between 661 and 742 mm (Figure 27 and Table 1) which is in the area of the thorax where the deflection sensors are most sensitive to impact height.

Another key dimension is the longitudinal distance between the ATD and the table. The Type IV table had a fairly large spacing to the forward-facing seatback (see Dimension A in Table 1) compared with the other tables that were tested. In most cases, it is preferable for the occupant to experience a larger proportion of the contact forces with the rear-facing seat bottom than the table since contact forces to the knee have not been shown to cause fatalities in rail accidents.

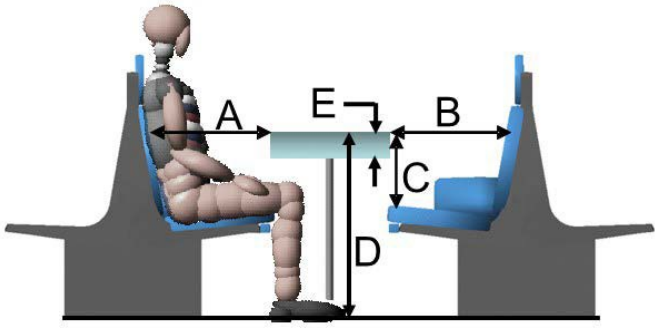

Figure 27. Sled Test Diagram Showing Key Dimensions

Table 1. Nominal Dimensions from Sled Test

Table Design	A	B	C	D	E
	mm	*mm*	*mm*	*mm*	*mm*
Type I	428	444	313	742	61
Type II	425	515	304	735	57
Type III	500	498	278	730	45
Type IV	505	536	294	725	64

The rigid body-spring FE model used in this study is a simplified representation of the actual energy absorbing table design. A detailed FE model of the table with deformable elements and calibrated material models would be a more accurate representation of the physical table and likely correlate better with test measurements; however, the authors were interested in studying whether it was possible to capture the chest and abdomen deflections measured by the ATDs using only the exterior dimensions of the table and the quasi-static test results from Option B of the APTA table standard to derive the table stiffness parameters. It was determined that this approach provided useful insight into the dynamics of the sled test.

Future work will also focus on: (1) fine-tuning the knee-to-seat contact to better capture the motion of and loads on the lower extremities; (2) investigating a deformable FE model of the Type IV table and comparing it with the rigid body-spring model; (3) modeling simplified representations of other table designs.

Once a validated model of the APTA 8G sled test is developed, further studies are planned to develop results that will help inform possible revisions to the APTA table standard.

ACKNOWLEDGMENTS

This work was performed as part of the FRA Office of Research, Development, and Technology Equipment Safety Research Program. The authors would like to thank the program manager Jeffrey Gordon. The authors would also like to thank Dr. Hubert Ley and Dr. Cezary Bojanowski at Transportation Research and Analysis Computing Center (TRACC) for access to their high performance computing cluster and Dr. Stephen Summers at NHTSA for access to LS-DYNA. Lastly, the authors would like to thank Marine Favre-Decloux and Michael Pittman at TRL for training in the use of the H3-RS FE model and arranging for the loan of the model respectively.

REFERENCES

[1] Rail Safety Standards Board, "Requirements for Rail Vehicle Structures," *GM/RT2100 Issue Five,* June 2012.

[2] American Public Transportation Association, "Fixed Workstation Tables in Passenger Rail Cars," APTA PR-CS-S-018-13, Rev. 1, October 2015.

[3] D. Hynd and C. Willis, "Sled Tests Using the Hybrid III Rail Safety ATD and Workstation Tables for Passenger," DOT/FRA/ORD-17/10, August 2017.

[4] S. Eshraghi, K. Severson, D. Hynd and A. B. Perlman, "Finite Element Model Validation of the Hybrid-III Rail Safety (H3-RS) Anthropomorphic Test Device (ATD)," in *ASME IMECE2018-87736*, Pittsburgh, PA, November 2018.

[5] K. Severson, A. B. Perlman, M. Muhlanger and R. Stringfellow, "Evaluation of Testing Methods to Develop Test Requirements for a Workstation Table Safety Standard," in *ASME Rail Transportation Division Fall Technical Conference*, Roanoke, VA, October 2010.

[6] M. Muhlanger, D. Parent, K. Severson and B. Perlman, "Development of Performance Requirements for a Rail Passenger Workstation Table Safety Standard," in *Rail Transportation Division Fall Technical Conference, RTDF2010-42031*, Roanoke, VA, October 2010.

[7] TASS International, "MADYMO Reference Manual V7.7," Helmond, Netherlands, 2017.

[8] K. Severson and D. Hynd, "Dynamic and Quasi-static Testing to Evaluate the APTA Table Standard," in *International Symposium on Passive Safety of Rail Vehicles*, Berlin, Germany, March 2017.

[9] D. Parent, D. Tyrell and B. Perlman, "Crashworthiness Analysis of the Placentia, CA Rail Collision," in *International Crashworthiness Conference*, San Francisco, CA 2004, July 2004.

[10] D. Parent, D. Tyrell, R. Rancatore and B. Perlman, "Design of a Workstation Table with Improved Crashworthiness Performance," in *ASME IMECE2005-82779*, Orlando, FL, November 2005.

[11] D. Tyrell, K. Jacobsen, D. Parent and B. Perlman, "Preparations for a Train-to-Train Impact Test of Crash-Energy Management Passenger Rail Equipment," in *Joint Rail Conference, RTD2005-70045*, Pueblo, CO, March 2005.

[12] SAE J211-1, "Instrumentation for Impact Test," Warrendale, PA, Revised March 1995.

[13] D. Hynd and J. A. Carrol, "Abdomen Impact Testing of the Hybrid III Rail Safety (H3-RS) Anthropomorphic Test," DOT/FRA/ORD-17/17, September 2017.